18

Electrochemical Co-deposition of Metal-Nanoparticle Composites for Microsystem Applications

Kyle Jiang
School of Mechanical Engineering, University of Birmingham, UK, B15 2TT

1. Introduction

Electrochemical deposition has been regarded as one of the key disciplines to microtechnology [1], as it provides a way to produce high precision microcomponents in various pure metals, alloys and composites in cost effective processes. Among the first microdevices demonstrated, were the electrochemical deposition of lithographically patterned features introduced in the early 1960's by IBM to increase memory density and reduce the physical size of memory devices [2]. The electrochemical deposition onto microfabricated template is also known as electrodeposition and microelectroforming in literature.

Electrochemical deposition is widely used for producing metallic components from sub-millimeters to a few millimeters in overall dimensions and up to a few hundred microns in thickness, i.e. in a range other metal deposition methods cannot challenge. As electrodeposition is particularly suitable for producing thick metallic microstructures, early efforts in this area were concentrated in producing relatively deep micromoulds. A renown process in this field is LIGA, pioneered in Germany in the early 1980s [3]. LIGA is the abbreviation of three German words representing three process steps, i.e. lithography (Lithographie), electroforming (Galvanoformung) and moulding (Abformung). It has been applied to fabrication of metallic microstructures and plastic replicates.

LIGA fabricated Ni microstructures and microcomponents have been applied in micro sensors and actuators. However, applications in harsh service conditions such as high temperature, high pressure, constant corrosion and friction put forward a requirement of better material properties on LIGA Ni, as numerous studies in characterizing LIGA fabricated samples have showed the insufficient mechanical and tribological properties of pure Ni. For example, Ni has been found to have high friction coefficient during the wear testing of LIGA fabricated microrotors [4]. It implies that Ni lifetime was well below the required level. The high friction coefficient of Ni also leads to problems in obtaining dimensionally accurate microcomponents with high aspect ratio during the plastic moulding process [5]. The stress-life experiments have shown that LIGA Ni structures have endurance limits that scale with tensile strength. [6].

Electroformed alloys and metal matrix composites (MMC) are promising alternatives to pure metals, which is proposed in literature for improving properties of LIGA Ni or replace Ni for microsystem applications. The former introduces alloy elements into Ni during electroforming process. For example, nanocrystalline nickel–tungsten (Ni-W) alloys are being considered as an attractive alternative to electroformed Ni for applications such as mould inserts and micro motors [7]. So far, however, only a few number of binary alloys, i.e. NiCu, NiFe, NiCo and NiP, have been attempted in LIGA fabrication of microstructures [8]. The latter introduces non-metallic particles usually to Ni matrix for improving the properties of the components. It is well documented in the literature that the solid and dispersed particulate composites possess a greatly enhanced mechanical properties compared with their metallic counterparts in strength, hardness, tribological properties and high temperature properties [9]. Recent research developments on nanomaterials provide scientists and engineers many new opportunities to synthesize nanocomposites with enhanced properties and design novel devices for microsystems. This chapter gives a brief introduction to this research with the latest results reported in literature.

2. Fabrication of Micromoulds in Photoresist

Central to the LIGA process is the fabrication of high quality LIGA moulds, and the X-ray sensitivity of thick resists is very critical to the LIGA process **Error! Reference source not found.**]. Polymethylmethacrylate (PMMA) was widely used in deep X-ray lithography initially. It is not highly sensitive to X-rays and a thick piece of PMMA sheet (>1mm) needs a long time to get exposed and results in excessive cost or fabrication difficulties **Error! Reference source not found.**]. In addition, the high costs for access to X-ray from a synchrotron limit the technique from wide applications. The commercial appearance of SU-8 in 90s started to change the situation. SU-8 is imageable with X-ray, UV and electron beam. Compared with PMMA, it requires much less exposure energy. In fabrication of 600µm standing microsctructures with X-ray exposure, PMMA requires a typical bottom dose of 4000 J/cm^3, while SU-8 requires 30 – 52 J/cm^3, only about a hundredth exposure energy of what PMMA requires [12]. Such high sensitivity to exposure proves sufficient even under UV exposure. Therefore, SU-8 photoresist gradually becomes the most popular resist for the LIGA process and UV-LIGA technique with wavelength of 356-405nm has been rapidly developed.

SU-8 is a negative tone, near-UV photoresist developed and patented by IBM in 1989 [13]. The photoresist is based on the EPON SU-8 epoxy resin from Shell Chemical. Depending on the percentage of the organic solvent and so the viscosity of the resist, the thickness of a single-spin SU-8 film can reach more than 500µm. SU-8 resist is well known for its excellent mechanical properties and low optical absorption in the near-UV range which results in uniform exposure conditions across the thickness [14] [15]. It has been reported that 1000µm thick microstructures with 40:1 aspect ratio was produced in a single lithography cycle [16] and a 1200µm thick microstructure with 18:1 aspect ratio in a double spin lithography process [17], both of which are of good vertical sidewalls and geometry. However, SU-8 is difficult to be stripped, and frequently, oxygen plasma process is required to remove SU-8 after electroforming. This property limits its applications to permanent components or micromoulds of only convex shapes most time. Meanwhile the needs for thick and strippable micromoulds lead to the development of some new resists.

Niedermann et al. [] presented DiaPlate 133 as a negative tone strippable photoresist for electroforming. A 60μm thick nickel foil with 32μm diameter holes and a 300μm thick nickel microgear were successfully electroformed using this resist. However, distortion seemed severe when the feature size was less than 50μm and a complicated long time soft bake is required when the thickness of the resist was greater than 200μm. Srinivasa Rao et al [] used JSR THB 151N resist, which requires a short time in soft baking, to develop 130μm thick and 2.6:1 aspect ratio electroforming moulds with near vertical sidewalls. Lee and Jiang [] studied KMPR, a photoresist newly developed by Microchem™, and microcomponents with an aspect ratio of 18:1 were fabricated.
BPR100 is another negative tone thick photoresist with a single-spin film thickness ranging from 40 to 130μm. It has been applied to a variety of electroplating and etching processes used in wafer level packaging. However, its dark blue colour absorbs irradiated beam energy, causing uneven exposure from top to bottom of a thick layer. This make it difficult to be used for thick moulds. The fabrication processes and the results of SU-8, KMPR and Shipley BPR 100 are presented as follows.

2.1 SU-8 Fabrication Process

SU-8 photoresist series have many grades for applications of different thickness. Take SU-8 2075 for example, it contains 73.45% solid and is intended for a thickness range from 75 to 225μm. In its process, the attention should be focused on softbake time and exposure dose for the optimum dimensional accuracy and sidewall profile of the microstructures. The processing parameters can be found in [21]. An optimized process for producing 500 μm thick SU-8 2075 moulds is used here as an example to introduce SU-8 process.
First, a 6ml SU-8 2075 photoresist is directly cast on a 4 inch silicon wafer coated with a thin layer of gold deposited by using thermal evaporation. After the photoresist spreads evenly, a soft bake at 65°C for 2 hrs and then 95°C for 8hrs is carried out on a levelled hotplate. The softbake step is performed to evaporate all the solvent in the resist and solidify the coated resist layer. UV exposure density is 12.6mW/cm^2. In the UV exposures, hard contacts are used between the SU-8 layer and the mask. A chrome mask is used in the exposure step. The total exposure dose is 3019mJ/cm^2. A postbake at 65°C for 2min follows and then 95°C for 20min. The polymerisation process occurs during the exposure and postbake steps. More specifically, the photoacid is generated in the resist during the exposure step and the crosslinking of epoxy groups takes place in the post bake step. The crosslinked SU-8 structures are then retained on the wafer after developing in the EC solvent for 10min.
Figure 1 shows an SU-8 mould for electroforming a microgear. Other SU-8 grades such as SU-8 2002, SU-8 2005 and SU-8 2050 are for different thicknesses. Their fabrication process are similar to SU-8 2075, but the processing parameters such as spin speed, baking time and exposure do need to be determined from experiments and optimised for each application case.

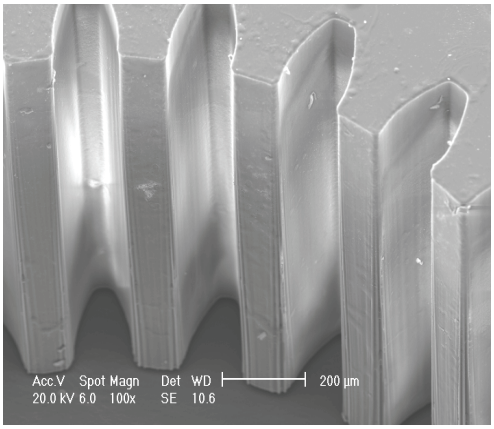

Fig. 1. SU-8 mould for producing microgears using electroforming.

2.2 Fabrication of KMPR micromoulds

KMPR photoresist is a chemically amplified negative tone epoxy photoresist. It was developed with the intention to resolve the stripping problem inherent with SU-8. Similar to SU-8, a KMPR process includes spin coat, prebake, exposure, post-exposure bake and development, and an additional resist stripping step is possible after electroforming. The particular KMPR series commercially available from MicroChem include 1005, 1010, 1025 and 1050 to cover thicknesses from 5 to 115 µm. More process details can be found from the MCC KMPR datasheet [22].

KMPR 1025 is taken as an example to demonstrate its process here. In a single layer lithography process, KMPR 1025 photoresist is first spun coated up to 60 µm thick on a metalized wafer and soft baked. If the required micromoulds are thicker than 60 µm, a multiple spin deposition can be applied. A multiple spin deposition process consists of spin deposition, soft bake, spin deposition and soft bake again, until the thickness reaches the requirement before the UV exposure, PEB and development steps.

In a single spin deposition process for making 60 µm KMPR photoresist layers, the following steps are used. (1) The spin deposition is conducted at 1000 rpm for 30 seconds. (2) The wafer is soft baked on a hotplate at 100oC for 20 mins. (3)Then the coated wafer is exposed to UV light at a density of 1135 mJ/cm2 using a chromium coated glass mask. The UV light source can be provided by a mask aligner with a wavelength range of 365 to 436 nm. (4) Post exposure bake (PEB) is carried out on a hotplate immediately after the exposure for 3 mins at 100°C. (5) The wafer is developed in 2.38% TMAH MF26A solution (Chestech, UK) for 6 mins in room temperature and the micromoulds should appear on the substrate. (6) Finally, the wafer is blown dry using N_2 gas. In a multiple layer deposition process, Steps (1) and (2) above will be repeated until the thickness reaches the requirement before moving to step (3). It is noted that the soft bake time for a multilayer deposition is different from that for a single layer. For the first layer, 100°C for 20 mins baking condition is adequate. However, for the second layer and onwards, 100°C for 30 mins baking time is more appropriate. The increase in baking time is understood as that the previous layer tends to soak some solution from the newly deposited resist and it takes longer time to evaporate the solution from the both layers.

Figure 2 illustrates an SEM image of a 180 μm thick micropiston mould made of KMPR. The resist was deposited in two spin and soft bake cycles, in which the spin deposition was carried out at 700 rpm for 30 seconds and the soft bake temperatures were at 100oC for 20 mins for the first layer and 30 mins for the second layer. The SEM images show that dimensions can be controlled at a high resolution and sidewall about in 90±1°.

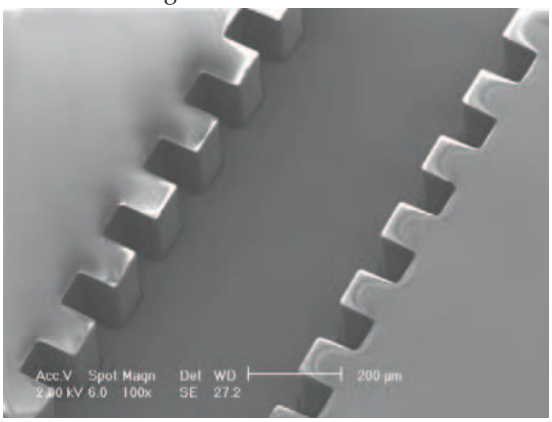

Fig. 2. An SEM image of a 180 μm thick KMPR photoresist moulds deposited using a multiple spin process.

2.3 BPR100 Fabrication Process

The fabrication process of BPR100 mould is slightly different from that of SU-8 and KMPR in that a post bake is not required before development. An optimized process of producing 100μm BPR100 micromoulds is introduced as an example.

A metalized substrate is first cleaned using acetone and isopropyl alcohol (IPA) separately. Then the substrate is pre-baked on a levelled hotplate at 120°C for 90s. After being naturally cooled down to room temperature, the substrate is spun coated with one layer of BPR100 photoresist. The coating consists of spreading spin and level spin. In the spread spin, the spin speed is ramped to 500 rpm at 100 rpm/second acceleration and held for 10 seconds. In the level spin, the speed is ramped to 800 rpm at 100 rpm/second acceleration and held for 30 seconds. This will result in a 100 μm layer. Further details for achieving different thickness can be found in [23]. A thicker layer can be achieved with a multilayer deposition process, involving repeated spin coating and baking cycle. After the photoresist had been coated, the substrate is soft baked to evaporate the solvent. This is done in two steps. First, the baking temperature is ramped from 20°C to 65°C at a rate of 5°C/min, held for 3 mins at 65°C, and then from 65°C to 95°C at the same rate, held for 7 mins at 95°C. After being cooled down, the baked substrate is then exposed using the same mask aligner for 80 seconds. The exposed substrate is subsequently developed in a solution of Eagle 2005 and deionized water in the ratio of 1:24 at 39°C for 5~10 mins depending on agitation of the developing solution. A hard bake is followed at 105°C for 5min. The resultant BPR100 moulds are examined using an SEM. Figure 3 shows two micromoulds made in Shipley BPR 100. The moulds are 200 μm deep and have straight sidewalls, providing excellent conditions for forming quality thick metallic components.

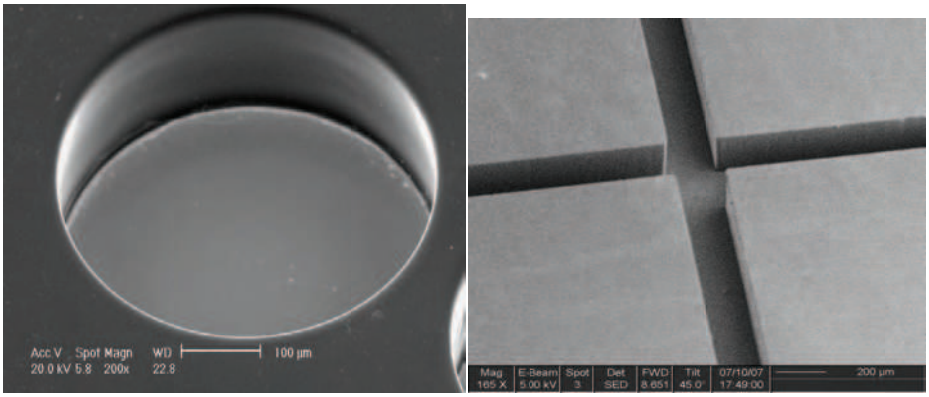

Fig. 3. Micromoulds made in Shipley BPR 100 resist.

3. Electrochemical co-deposition of metal/nanoparticles

3.1 Electrochemical Deposition

In a typical electrodeposition setup, shown in Figure 4, two electrodes are submerged in a plating solution. One of the electrodes is the anode, linked to a block of the source metal, while the other is the cathode, linked to the micromoulds with areas to be deposited with the metal. The two electrodes are powered by an external power supply. The plating solution is a salt of the metal for deposition. For Nickel deposition, nickel sulfamate solution is used, which consists of nickel (85~95g/L), nickel chloride (8~12g/L) and boric acid (25~35g/L).

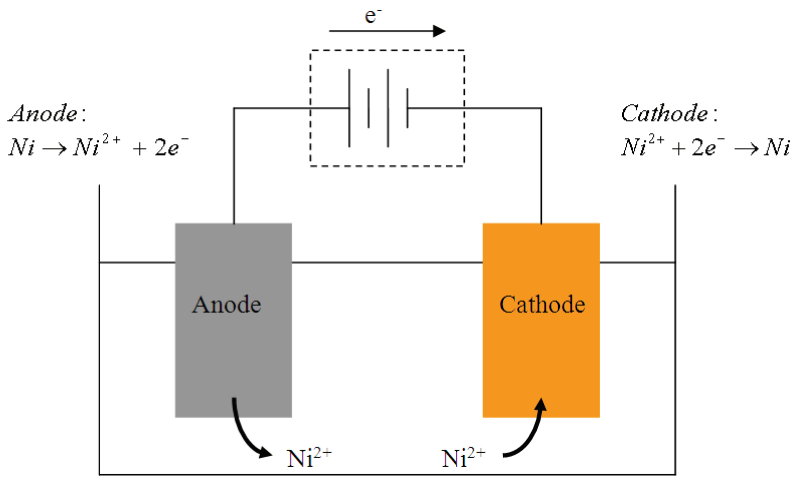

Fig. 4. Schematic representation of an electrodeposition cell

The mechanism of how a cation merges with an electron from the cathode to form a metal atom on the substrate is arguable in two main theories [24]. According to one theory, the cation is discharged and neutralised preferentially in to an active site on the substrate. If

there is no active site within a distance for the cation to discharged, a new nucleus is formed. This theory postulates a lower potential is needed for the cation to grow on an existing crystal than to create a new crystal [24]. The other theory suggests that the cation is neutralised and discharged at random, and form into a metal atom on the surface of the substrate. The metal atoms then orient themselves into the lattice and grain size that is characteristic to the metal. This theory assumes that the discharged metal atoms have the appropriate mobility [24].

In electroforming practice, the usual problems are air bubbles, uneven growing of deposited metal and grain size control. Continuous research has been conducted in this arer for improving the quality of deposition. Apart from improving agitation conditions, including using ultrasonic agitator, pH and temperature control, and small additives, the configurations of the electrodeposition, such as Hull cell, and variations on voltage patterns have been explored, and good results have been achieved for particular applications. Further reading can be found in references [25, 26, 27, 28].

3.2 Nanoparticles and their preparation for electrochemical co-deposition

Composite materials provide a useful way to change the properties of the materials. Electro co-deposition of nanoparticles with metals is one of the recent developments in electroforming field. The micro composite components often demonstrate superior properties. Ceramic nanoparticles are widely adopted as the fillers and they are commercially available. For example, fumed Al_2O_3 nanoparticles of high purity can be purchased from CABOT Cooperation™.

It is well known that the nanoparticles tend to agglomerate into clusters due to their high surface energy. The phenomena can be observed in SEM analysis. A small amount of Al_2O_3 nanoparticles is first diluted in DI water and dispersed using a mechanical stirrer for 30 mins. An ultrasonic agitation of the Al_2O_3 suspension is followed for 15 mins. A little of diluted Al_2O_3 suspension is dropped on a metal stub and dried up slowly. After gold sputtering, the prepared sample can be examined under the SEM microscope. It can be seen from Figure 5 that the nanoparticles are still agglomerated to some extent and the particle size is estimated to be around 30 nm. The HRTEM micrograph in Figure 6 indicates that the nanoparticle size is in the range from 25nm to 50nm.

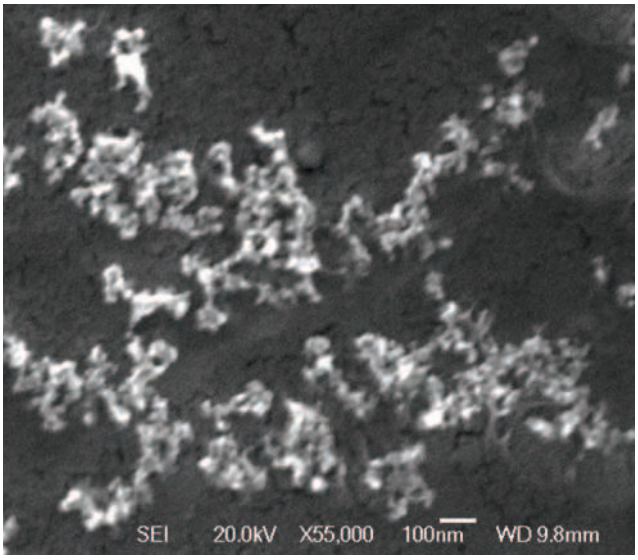

Fig. 5. High magnification SEM micrograph of Al_2O_3 nanoparticles

Nanoparticles should be well dispersed in the electrolyte in order to achieve uniform distribution in the metal matrix. Therefore, it is necessary to avoid agglomeration of nanoparticles in the solution as much as possible. For this reason, the dispersion property of the nanoparticles in the nickel electrolyte was investigated by performing zeta potential measurements. The tests were carried out in a Zeta Potential Analyzer (Zetamaster, Malvern instruments, U.K.). The suspension was diluted to 0.2g/L by DI water and the pH value was adjusted with NaOH and HCl. The obtained results will be present and discussed in the next section.

In the composite electroforming processes, the Al_2O_3 nanoparticles is firstly dispersed in the DI water using a mechanical stirrer for 30mins and then the suspension is ultrasonically agitated for 15mins. After the nickel sulfamate electrolyte is heated to the desired temperate, the Al_2O_3 suspension was slowly mixed into the electroforming bath, which is agitated continuously using a magnetic stirrer. The prepared composite bath is maintained at the constant temperature and agitation for about 30mins prior to electrodeposition. The loading of Al_2O_3 nanoparticles in the bath, operating temperature and the current density have been studied to find the effects of electroforming conditions on the properties of electroformed microcomponents.

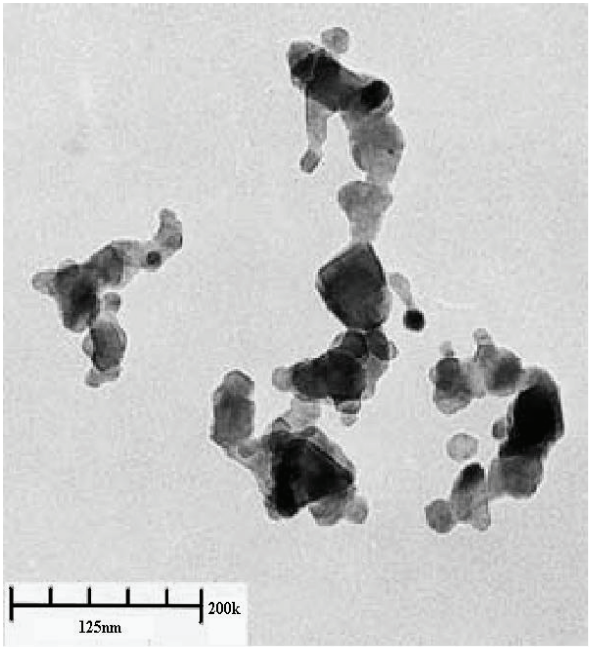

Fig. 6. HRTEM image of Al_2O_3 nanoparticles used in this study (By courtesy of CABOT Cooperation™)

Carbon nanotubes have been co-deposited into Ni matrix, together with Al_2O_3 nanoparticles, as reported by Wei and Jiang [29]. A commercial nickel sulfamate solution (PMD Chemicals Ltd, UK) was used as the host electrolyte for preparing the nickel and nanoparticles colloidal bath. Al_2O_3 nanoparticles (SpectrAl™ 81) of a high purity and raw Multi-Walled Carbon Nanotubes (MWCNTs) were used as the second phase materials for the composite deposition. First, Al_2O_3 nanoparticles and MWCNTs were added into two beakers containing nickel sulfamate electrolyte. However, the nanoparticles and CNTs tend to agglomerate due to the Van Der Walls force. Besides, the hydrophobic nature of CNTs makes them difficult to dissolve in most solutions. Sodium dodecyl sulphate (SDS) as a surfactant was used to improve the dispersion of nanoparticles and CNTs in the solution. Then, the two beakers of colloidal solution were placed in an ultrasonic bath agitation for 30 minutes before mixing the solutions in one beaker. In order to improve the contact between the Al_2O_3 nanoparticles and MWCNTs, the mixture was alternatively agitated using the ultrasonic and mechanical stirring methods for a total of 30 mins before conducting any experiment. Table.1 shows the composition of the prepared electrodeposition bath.

Symbol	Name	Value
$Ni(NH_2SO_3)_2$	Nickel Sulfamate	380~425g/L
$NiCl_2$	Nickel Chloride	8~12g/L
H_3BO_3	Boric Acid	25~35g/L
$NaC_{12}H_{25}SO_4$	Sodium Dodecyl Sulphate	~1g/L
Al_2O_3	Alumina Nanoparticles	3g/L
MWCNTs	Multi-Walled Carbon Nanotubes	0.05~0.3g/L

Table 1. Composition of the bath for Ni-Al_2O_3/CNTs electrodeposition.

A study on their dispersion behaviour in the nickel sulfamate bath was conducted. It was found that the addition of SDS makes the dispersion of Al_2O_3 nanoparticles and MWCNTs easier with the aid of sonication. Zeta potential measurements of the diluted solution taking from the prepared nickel composite bath show that the surfaces of Al_2O_3/MWCNTs are positively charged in the pH value of a wide range from 2 to 14. Therefore, Al_2O_3 nanoparticles and MWCNTs will migrate to the cathode in the electrical field.
The experiments were performed in a 1L glass beaker using a potentiostat/galvanostat power supply (TENMA^{TM} 72-6153). A magnetic stirrer was used to agitate the bath to keep the solution with a uniform concentration and reduce the agglomeration of nanoparticles and CNTs during the experiments. The current density was varied in the range of 10~50mA/cm^2. The temperature and pH were maintained at 50±2^oC and 4.3±0.1 respectively during the experiments.

3.3 Analysis of microstructures, surface morphology and composition

After electrodeposition, the resultant microcomponents were ultrasonically cleaned in deionized water for 30s to get rid of the loosely attached Al_2O_3 nanoparticles and MWCNTs. The surface morphology was characterized using a scanning electron microscope, and the content of nanoparticles and MWCNT incorporated in the Ni matrix was evaluated from the aluminium and carbon signals using Energy Dispersive X-ray Spectroscopy (EDX) coupled with the SEM. Microhardness tests were conducted in a hardness machine (MVK-H1, Mitutoyo) using a load of 100g force and a dwelling time of 15s.
Fig. a shows an SEM image of a micro gear electrodeposited from a bath containing 0.05g/L MWCNTs and 3g/L Al_2O_3 nanoparticles. Clearly, the gear is uniformly grown through the SU8 micromould and its sidewalls are very smooth, while its top surface morphology is distinct from that of electroformed pure Ni, as shown in Figure 7b. The previous study has shown that the peaks of nickel pyramids are round and even flat in the co-deposition of Ni-Al_2O_3 nanocomposite. However, unlike Al_2O_3 nanoparticles, CNTs are electrically conductive material. Hence, the embedment of MWCNTs on the cathode surface enlarges the electrodeposition area, and accordingly leads to a spherical growth of deposit. Even a low MWCNT loading in the bath still shows its effects as observed in Figure 7b. Increasing the MWCNT loading in the bath enhances the trend of spherical growth of the deposit.
Figure 8 shows a surface of a micro gear electroformed from a bath containing 0.3g/L MWCNTs and 3g/L Al_2O_3 nanoparticles. It can be seen that the surface is very rough and

there are lots of micro gaps. It was also found that the two ends of MWCNTs are embedded in the nickel matrix and other parts of tube are above the nickel surface attached by Al_2O_3 nanoparticles as shown in the micrograph of a high magnification, Fig9. This could be explained as that CNTs have a high electrical conductivity along their axial direction, and therefore, the tube ends of CNTs are easily deposited in the nickel matrix during the deposition process. The high curvature of nanotubes leads to high surface energy of carbon atoms, which makes MWCNTs surface attract Al_2O_3 nanoparticles. The density of applied current has a dramatic effect on the morphology of the deposit, as it is found that a high current density will lead to breakdown of the uniform growth of the deposit, forming a very rough surface. A low current density was therefore used in the experiments to fabricate microcomponents.

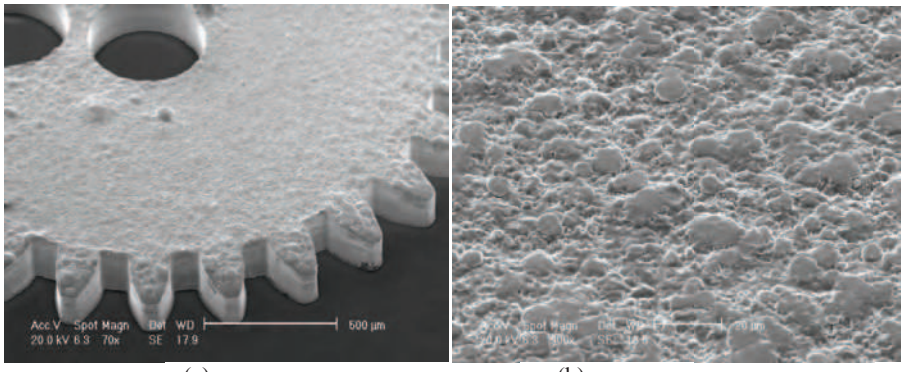

(a) (b)

Fig. 7. (a) An SEM image of a microgear deposited in a nickel sulfamate solution containing 0.05g/L MWCNTs and 3g/L Al_2O_3 nanoparticles. (b) A zoomed view of its surface morphology.

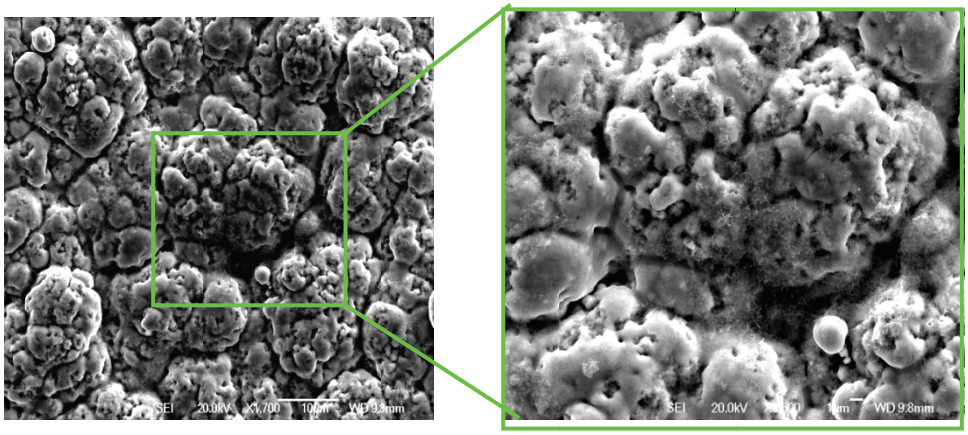

Fig. 8. SEM micrographs of Ni-Al_2O_3/MWCNTs Nanocomposite surface morphology

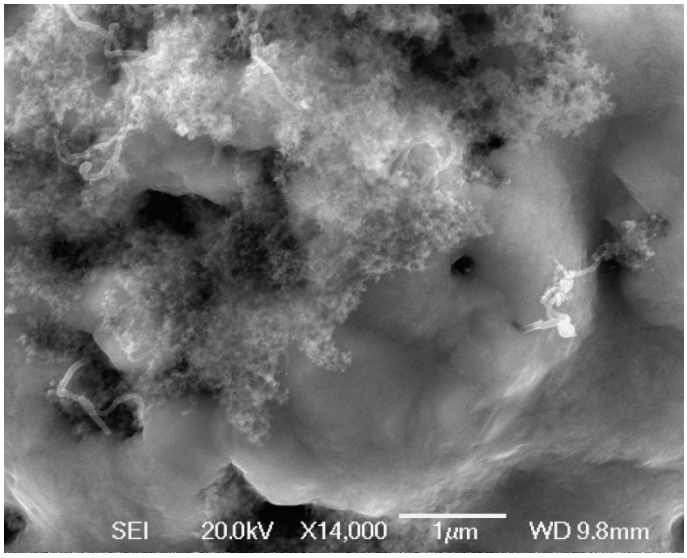

Fig. 9. An SEM Micrograph of Ni-Al_2O_3/MWCNTs Nanocomposite in high magnification

The content of Al_2O_3 nanoparticles in the nanocomposite is affected by the bath composition and electroforming conditions. Figure 10 shows a spectrum of EDX examination on the surface of Ni-Al_2O_3/MWCNTs nanocomposite. It was found that the average volume percentage of Al_2O_3 embedded in the nanocomposite electroformed from a bath containing 3g/L nanoparticles is around 9±2.5%. The average volume percentage of embedded Al2O3 electrodeposited from a bath containing 3g/L Al2O3 nanoparticles and 0.05g/L MWCNTs is around 6.65%. The results of EDX examination and x-ray mapping indicate that the nanoparticles are uniformly distributed in the Ni matrix. As expected, the higher the concentration of Al_2O_3 nanoparticles in the bath, the more nanoparticles are incorporated into the composite electroform with no observed tendency to precipitation.

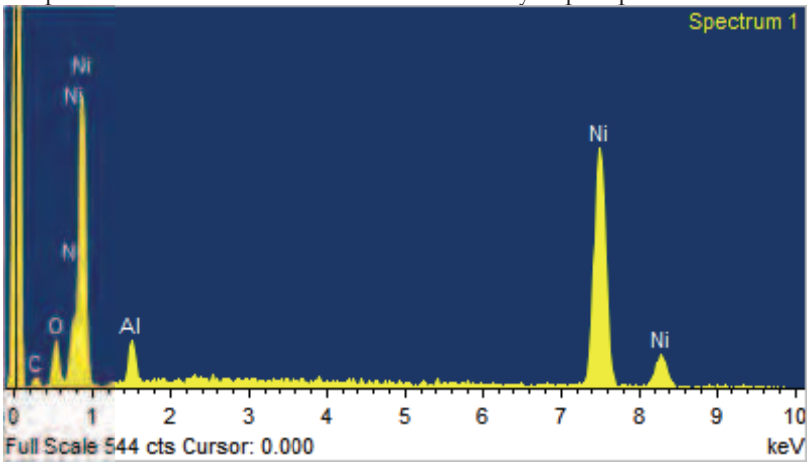

Fig. 10. Energy dispersive spectrum of Ni-Al_2O_3/MWCNTs nanocomposite.

4. Mechanical properties of nanocomposites

4.1 Microhardness

As many factors influence the hardness of electroformed Ni-Al_2O_3 microcomponents, a systematic study was carried out to investigate the effects of the major factors, such as temperature, current density and loading of Al_2O_3 nanoparticles. In this study, the microhardness of the Ni-Al_2O_3 nanocomposite electrodeposited at 45°C and 55°C respectively with the similar pH and current density was compared. It was found that the lower temperature and higher current density result in a relatively higher hardness as shown in Fig. 11. The hardness of deposits usually falls with the rise in temperature of the plating conditions. It can be explained that increasing temperature will lead to high cathodic overpotential, which favours the formation of fine grains and therefore results in high hardness.

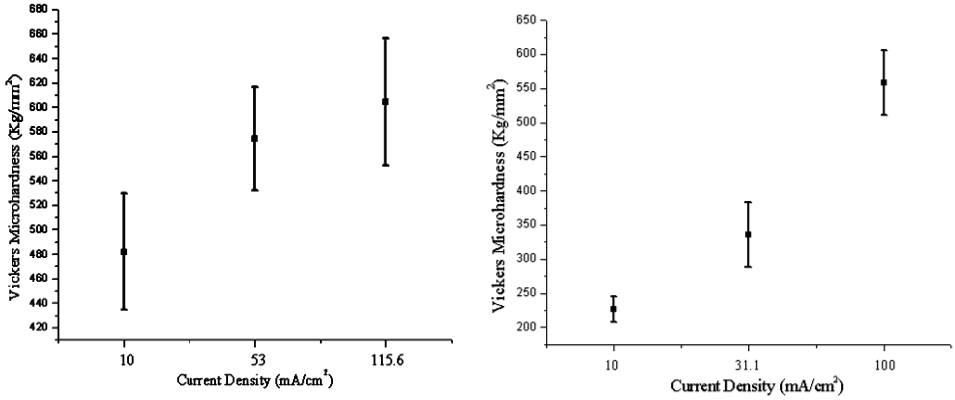

Fig. 11. Microhardness of nanocomposites made from (a) 45°C and (b) 55°C respectively at the similar pH value and current density.

For the high temperature applications, the effect of post heat treatment on mechanical strength of Ni-Al_2O_3 composite was characterized by using a microhardness tester. Ni-Al_2O_3 microcomponents were electroformed using a current density of 25mA/cm^2 from the bath containing 20g/L Al_2O_3 nanoparticles. After stripping off the photoresist moulds, microcomponents were treated in a vacuum heating furnace with a vacuum pressure of 10^{-5}Pa. The applied temperature was gradually ramped up to 600°C at a ramping rate of 5°C/min and then it was cooled down to room temperature slowly after dwelling at 600°C for 1hr. Microhardness tests were performed on the post treated samples and the hardness was found $HV_{0.2}$ 300, which is still higher than that of electroformed pure nickel. It was found that a higher annealing temperature softened the Ni-Al_2O_3 nanocomposite while a relatively lower annealing temperature less than 200°C almost had no obvious effects on the microhardness of the sample. In comparison between the electroformed pure Ni and Ni nanocomposites, it can be concluded that the annealing effect is minimized due to the existence of Al_2O_3 nanoparticles, which hinders the nickel grains from growing bigger during the annealing process [31].

4.2 Elastic property

Since the appearance of LIGA technology, Ni as a MEMS material has been widely used, but its mechanical properties were not paid much attention only until the recent 10 years. Measurements of mechanical properties of electroplated or LIGA-deposited Ni now have been extensively conducted by many researchers using different techniques. The reported Young's moduli range from 148.04GPa ~ 159.90GPa by Kim [32], 175±7GPa by Ballandras *et al* [3], and 190.5GPa by Zhou *et al* [4]. Apart from the difference of methods they used, the Young's modulus of electrodeposited Ni is also strongly influenced by the fabrication conditions, including the temperature and current density. Luo *et al* Fig.[5] and Fritz [6] investigated the effects of temperature and current density in electrodeposition. They both found that Young's modulus decreased with respect to increasing the mean current density. In Figure 12, the Young's moduli of Ni reported in references [35] and [36] are compared with that of Ni–Al_2O_3 nanocomposite obtained from bending and nanoindentation tests in this study.

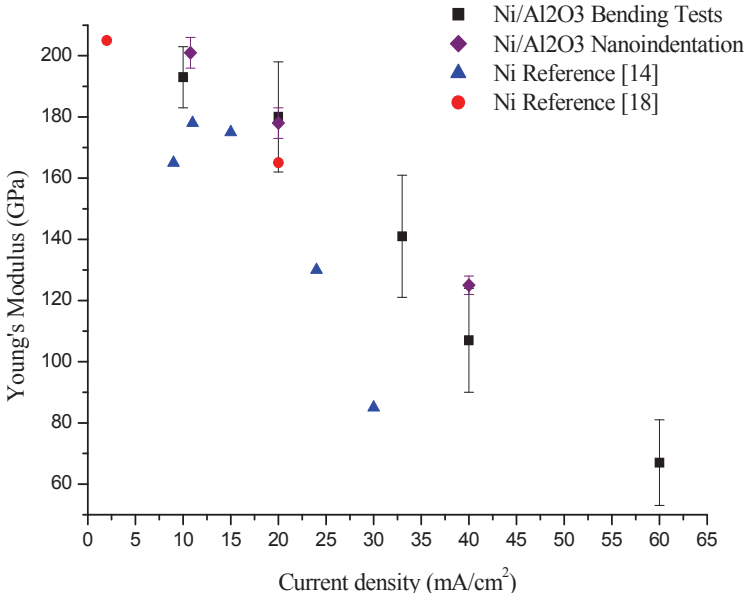

Fig. 12. Comparison of Young's Modulus of electrodeposited pure Ni and Ni–Al_2O_3 nanocomposite at different current density

It is found that the Young's modulus of Ni–Al_2O_3 nanocomposites is dramatically affected by the current density. Nevertheless, Ni–Al_2O_3 nanocomposite still has an increased elastic property than the pure Ni thin films as indicated in the comparison. According to the well-known rule of mixtures [7], such an enhancement is likely due to the addition of Al_2O_3 nanoparticles, which have a higher Young's modulus of roughly 300GPa. In addition, the Al_2O_3 nanoparticles also influence the growth of microstructures of the nickel matrix in the course of electroforming process, which will accordingly affect the intrinsic property, such as the Young's Modulus.

5. Examples of potential applications

Nickel has been used as a dominant metal in LIGA technology for over twenty years, and accordingly research on strengthening nickel properties by incorporating particles into nickel matrix is expected to improve the serving performances of microdevices and microcomponents made of pure nickel.

Teh and co-workers [8] proposed that the incorporation of diamond nanoparticles into nickel matrix formed in electroless electroforming to enhance greatly the overall stiffness of the nickel film attributed to the extreme hardness, stiffness, and temperature resistance of the diamond particle. As more diamond nanoparticles are incorporated into the matrix, the residual stress in the composite film is reduced, making it more suitable for fabricating suspended microstructures. It was found that an electrothermal microactuator made of Ni-nanodiamond composite film could reduce the power requirement by 73% from 0.924 to 0.248W, compared with a pure nickel device for the same 3μm displacement. In addition, the nanocomposite microactuator can exhibit reversible displacement over 3μm, which is larger than pure nickel one for only with 1.8μm displacement [9]. The authors then further investigated the effects on the performance of electrothermal microactuators deposited by the incorporation of diamond nanoparticles in nickel electrolytic bath, in terms of the mechanical strength, coefficient of thermal expansion (CTE) of the nanocomposite material, and the improvements of power consumption and operational reliability in the devices [40]. Similar effects were also found in the Ni-Cordierite nanocomposite thin film by these researchers [41]. The as-deposited nickel-cordierite films exhibit better thermal compatibility with silicon than nickel. The addition of cordierite particles significantly reduces the residual stress as shown in Figure 13. The inset shows a magnified view of the released double folded beam.

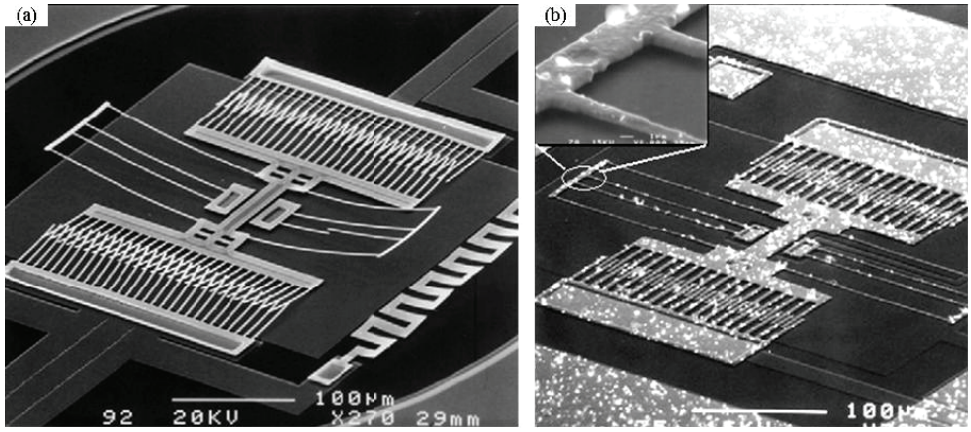

Fig. 13. (a) A partially released, internally stressed nickel microresonator; (b) A fully released, unannealed, residual stress free, nickel-cordierite microresonator

Wang and co-workers [2] fabricated Ni–Al_2O_3 micro pillars using PMMA moulds and the conventional nickel sulfamate bath containing Al_2O_3 particles. In the process, they monitored the changes of current density for pure Ni and Ni–Al_2O_3 deposition. It was found that the

addition of the particles in the plating bath causes the deposition process to change from mass transport controlled to partially kinetic controlled. This is reasonable because Al_2O_3 particles are non-conductive and their distribution in the vicinity of the cathode and their embedment in the deposit affect the reduction process of nickel ions. They also found that the deposition rate decreased as compared to the theoretical prediction. Fig. 14.14 shows an array of Ni–Al2O3 micro pillars (500μm tall and 200μm diameter) electrodeposited from a bath containing 7g/l Al2O3 particles. Results of mechanical tests showed that microhardness was substantially improved with the incorporation of particles. Following the same route, they also studied other MMC microcomponents, for example, Ni–SiC , NiCo–SiC and NiCu–Al_2O_3.

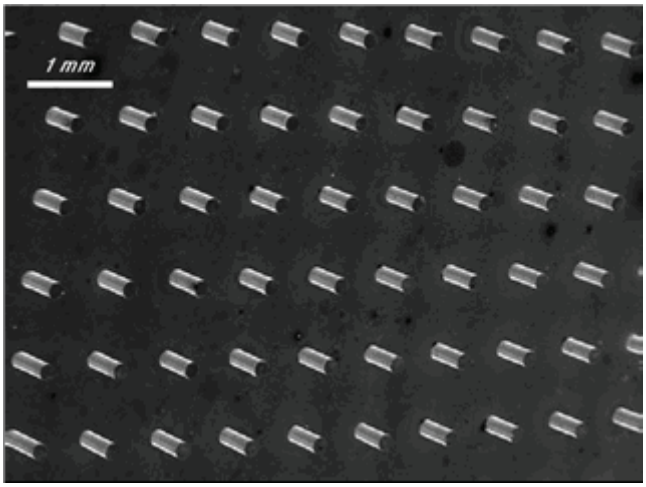

Fig. 14. Ni–Al_2O_3 posts grown from a bath containing 7g/l Al_2O_3 particles

It was found that the average volume percentage of Al2O3 embedded in the nanocomposite electrodeposited from a bath containing 3g/L Al2O3 nanoparticles and 0.05g/L MWCNTs is around 6.65%. The results of EDX examination and x-ray mapping indicate that the nanoparticles are uniformly distributed in the Ni matrix. The microhardness of the Ni-Al2O3-MWCNT composite microcomponents is found in the range of $HV_{0.1}$ 350~400. This value is greater than that of a pure Ni microcomponent produced from a similar bath without nanoparticles ($HV_{0.1}$ 280 ~ 330).

Wei and Jiang [29] fabricated Ni-Al_2O_3 microcomponents for a micro engine. Figure 7a is a composite microgear of Ni, Al_2O_3 and MWCNT for the device. The composition and mechanical properties have been discussed above. Figure 15 shows a Ni-Al_2O_3 composite micropiston for the microengine. It was electrodeposited from a bath containing 7g/l Al_2O_3 particles. The improved hardness of the nanocomposite Ni components will reduce the wear and extend the life, which is important in the design of microengines.

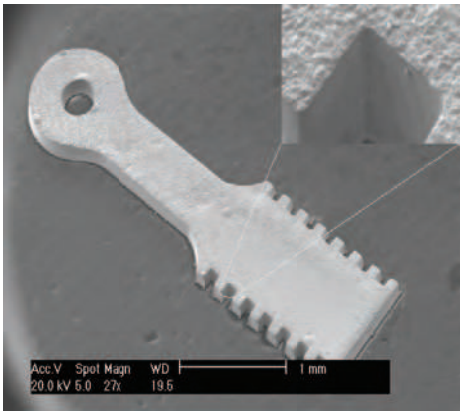

Fig. 15. A micro Ni–Al_2O_3 piston electroformed from a bath containing 7g/l Al_2O_3 particles.

Compared with nickel which has been widely used as a structure material for building up microcomponents and devices, copper is mainly used as a material for electronic interconnections and electrical microdevices. Gan and co-workers [43] studied the feasibility of electrodepositing copper matrix nanocomposite with Al_2O_3 nanoparticles onto silicon wafers. They successfully fabricated a microchannel array of Cu–Al_2O_3 nanocomposite as shown in Figure 16. Microstructural examination and nanoindentation experiments were performed on the nanocomposite. It was found that the presence of the Al_2O_3 nanoparticles in the bath interfere with the grain growth process during the electrodeposition and accordingly lead to smaller grain size compared with pure copper. The mechanical tests showed that the microhardness increased from 1.29GPa to 1.62GPa with the addition of the nanoparticles, which is a 25% increase.

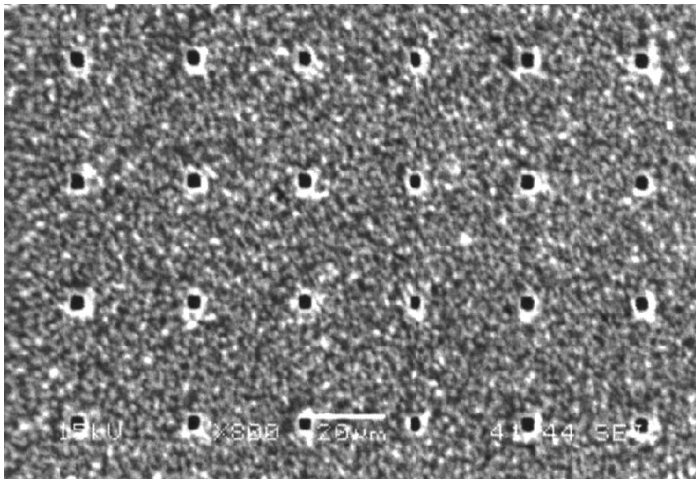

Fig. 16. vertically aligned microchannels in the Cu–Al_2O_3 nanocomposite film

6. Summary and conclusions

Electrodeposition of microcomponents is suitable for mass fabrication of high precision metallic microcomponents. Recent research has combined electrodeposition with nanomaterials and produced nanocomposite components. The research results currently available have demonstrated obvious advantages of the new development. This chapter introduces the latest nanocomposite electrodeposition techniques, characterization results and some applications.

After a general introduction to electrodeposition, the chapter presents the processes of producing high quality and thick micromoulds using three photoresists in SU-8, KMPR and Shipley BPR 100. SU-8 has been used for making moulds of over 1 mm in depth using UV exposure, but it may be difficult to strip. Oxygen plasma is widely used to remove the SU-8 moulds after metal deposition. KMPR was designed with the intention to overcome the stripping difficulty in electrodeposition applications. So far, the reported thickness of the moulds exposed using UV is limited to a few hundred microns. Shipley BPR 100 is another thick photoresist. Its dark blue colour absorbs irradiated light, making an even exposure through a thick layer very difficult. So far the reported thickness of Shipley BPR 100 layers is limited to about 200 μm. However, Shipley BPR 100 moulds can be completely dissolved, which makes it attractive for making relatively thin structures.

Setting and material preparation for nanocomposite co-deposition are introduced. Al_2O_3 nanoparticles and MWCNT have been used as the fillers. The proposed treatment of the nanomaterials against agglomeration in electrodeposition is proven effective. The co-deposited components have been examined. Because of the composite materials, the top of the components is a bit bumpy, but the side walls are smooth. Microstructure analysis shows that carbon nanotubes have been deposited into the structure in separate distribution. EDX analysis shows that the average volume percentage of Al_2O_3 embedded in the nanocomposite electroformed from a bath containing 3g/L nanoparticles is around 9±2.5%. The composite components have been analysed in term of hardness and elastic property. Overall, nickel composite is found harder than pure nickel. In addition, the deposition conditions are related to the hardness. It is found that lower temperature and higher current density result in a relatively higher hardness. Young's modulus of the composite components are generally higher than pure electrodeposited nickel. However, low deposition current resulted in higher Young's modulus.

The chapter provides some practical applications of the co-deposited nickel composite components, ranging from microresonators to microengines. In these applications, the microcomposite components show some excellent properties in thermal expansion, hardness, and wear resistance. These properties vary with the percentage of embedded naoparticles, which makes the composite components tuneable to suit their applications. Currently, the technology for electrochemical co-deposition of Ni-nanoparticles is just emerging, but it has demonstrated its obvious advantages for various applications. This technology has potential to be much developed to suit wide engineering applications.

7. References

[1] Wolfgang Ehrfeld, Electrochemistry and microsystem, Electrochimica Acta, 48 (2003) 2857-2868.

[2] L.T. Romankiw, A path: from electroplating through lithographic masks in electronics to LIGA in MEMS, Electrochimica Acta, 42 (1997) 2985-3005.
[3] E.W. Becker, W. Ehrfeld and et al., Production of separation-nozzle systems for uranium enrichment by a combination of X-ray lithography and galvanoplastics, Naturwissenschaften, 69 (1982) 520.
[4] T. Bieger and U. Wallrabe, Tribological investigations of LIGA microstructures, *Microsyst. Technol.,* 2 (1996) 63–70.
[5] Z. Peng, L. Gang, T. Yangchao and T. Xuehong, The properties of demoulding of Ni and Ni-PTFE moulding inserts, Sens. Actuators A: Phys. 118 (2005) 338–341.
[6] S. M. Allameh, J. Lou, F. Kavishe, T. Buchheit and W. O. Soboyejo, An investigation of fatigue in LIGA Ni MEMS thin films, Materials Science and Engineering A, 371 (2004) 256-266.
[7] A.S.M.A. Haseeb, U. Albers and K. Bade, Friction and wear characteristics of electrodeposited nanocrystalline nickel-tungsten alloy films, Wear, 264 (2008) 106-112.
[8] J. Hormes, J. Gottert, and et al, Materials for LIGA and LIGA based microsystems, Nuclear Instruments and Methods in Physics research B, 199 (2003) 332-341.
[9] R. K. Everett and R. J. Arsenault, Metal Matrix Composites: Mechanisms and Properties, Academic Press Limitted, 1991.
[10] E. W. Becker, W. Ehrfeld and et al, Fabrication of microstructures with high aspect ratios and great structural heights by synchrotron radiation lithography, galvanoforming, and plastic molding (LIGA process), Microelectronic Engineering, 4 (1986) 35.
[11] W. Ehrfeld, V. Hessel, H. Lowe, Ch. Schuiz and L. Weber., Materials of LIGA technology, Microsystem Technologies, 5 (1999) 105-112.
[12] L Singleton; A L Bogdanov., S S Peredkov, O Wilhelmi, A Schneoder, C Cremers, S Megtert, A Schmidt, Deep X-ray lithography with the SU-8 resist, Proceedings of Emerging Lithographic Technologies V, vol. 4343, pp. 182-192, 2001.
[13] H. Ito, CG. Willson, in: Proceedings of the SPE Regional Technical Conference on Photopolymers, Society of Plastic Engineers, 1982, p. 331.
[14] Lorenz H, Despont M, Fahrni N, LaBianca N, Renaud P and Vettiger P, SU-8: a low-cost negative resist for MEMS, J.Micromech. Microeng, 7 (1997) 121– 124.
[15] Lorenz H, Laudon M and Renaud P, Mechanical Characterization of a New High-Aspect-Ratio Near UV-Photoresist, *Microelectronic Engineering*, 41 (1998) 371 - 374.
[16] K. Jiang, M. J. Lancaster, I. Llamas-Garro and P. Jin, SU-8 Ka-Band Filter and Microfabrication, *J. Micromech. Microeng.,* 15 (2006) 1522-1526
[17] Lorenz H, Despont M and et al, High-aspect-ratio, Ultrathick, negative-tone near-UV photoresist and its applications for MEMS, *Sensors and Actuators* ,64 (1998) 33-9
[18] Niedermann Ph, Berthou H and et al. A novel thick photoresist for microsystem technology, *Microelectronic Eng*, 67-68 (2003) 259-265
[19]Rao VS, Kripesh V and et al, A thick photoresist process for advanced wafer level packaging applications using JSR THB-151N negative tone UV photoresist *J. Micromech. Microeng*. 16 (2006)1841-6
[20] Lee, CH and Jiang K, Fabrication of thick electroforming micro mould using KMPR negative tone photoresist, *J. Micromech. Microeng*., 18 (2008) 055032.

[21] K. Jiang, M. J. Lancaster, I. Llamas-Garro and P. Jin, SU-8 Ka-Band Filter and Microfabrication, J. Micromechanics and Microengineering, 15, 1522-1526, 2005
[22] Microchem and Nipon Kayaku, KMPR 1000 Guidelines,
[23] Rohm and Haas Electronic Materials, BPR 100 ™ Photoresist, http://www.sts-israel.com/files/pdf/BPR-100_PF04N022R1.pdf, August 2004
[24] Gray, A.G., Modern Electroplating. 1953, New York: London : John Wiley & Sons ; Chapman & Hall. 563p.
[25] R. Yu. Bek, T. P. Aleksandrova, and L. I. Shuraeva, Dependence of the Rate of Electrodeposition of Metals at Mono- and Multielectrodes on Voltage in the Case of an Exaltation Mechanism of Mass Transport, Russian Journal of Electrochemistry, Vol. 41, No. 10, pp. 1027–1031, 2005.
[26] B Marquardt1, L Eude1, M Gowtham1, G Cho1, H J Jeong1,MChâtelet1, C S Cojocaru1, B S Kim2 and D Pribat1, Density control of electrodeposited Ni nanoparticles/nanowires inside porous anodic alumina templates by an exponential anodization voltage decrease, Nanotechnology, 19 (2008) 405607
[27] R.O. Hull, Journal of American Electroplating Society, 27 (1939) 52-60.
[28] T.D. MCCOLM and J.W. EVANS, A modied Hull cell and its application to the electrodeposition of zinc, Journal of Applied Electrochemistry 31: 411-419, 2001.
[29] Xueyong Wei1 and Kyle Jiang, "Synthesis and characterization of nanoparticulate strengthened nickel microcomponents", Advances in Science and Technology Vol. 54, pp 299-304, 2008
[30] X. Wei, Z. G. Zhu, P.D. Prewett and K. Jiang, Microelectronic Engineering, Vol.84, (2007), p.1256-1259.
[31] C. S. Lin, C. Y. Lee, C. F. Chang and C. H. Chang, Annealing behavior of electrodeposited Ni-TiO2 composite coatings, Surface and Technology, 200 (12-13) 3690-3697, 2006.
[32] S. H. Kim, Determination of mechanical properties of electroplated Ni thin film using the resonance method, Mater. Lett., 61 (2007) 3589-3592.
[33] S. Ballandaras, S. Basrour, and et al. Microgrippers fabricated by the LIGA technique, Sensors and Actuators, A, 58(1997): 265.
[34] N. M. Zhou, Y. Zhou and et al., The evaluation of Young's modulus and residual stress of nickel films by microbridge testings, Measurement Science and Technology, 15 (2004): 2389.
[35] T. Fritz, M. Griepentrog and et al, Determination of Young's modulus of electroplated nickel, Electrochimica Acta, 48 (2003) 3029 - 3035
[36] T. W. Clyne and P. J. Withers, An introduction to metal matrix composites, London: Cambridge University Press, 1993
[37] T. W. Clyne and P. J. Withers, An introduction to metal matrix composites, London: Cambridge University Press, 1993
[38] K. S. Teh, Y. T. Cheng and L. W. Lin, Nickel nanocomposite film for MEMS applications, in Proc. 12th International Conference on Solid State Sensors, Actuators and Microsystems, Boston, MA, 2003, pp. 1534–1537.
[39] L. N. Tsai, G. R. Shen, Y. T. Cheng, and W. S. Hsu, The 54th Electronic Components and Technology Conference, June 2004, pp. 472–476.

[40] L. N. Tsai, G. R. Shen, Y. T. Cheng, Performance improvement of an electrothermal micro actuator fabricated using Ni-Diamond nanocomposite, Journal of MEMS, 15 (1) 149-158, 2006.

[41] K.S. Teh, Y. T, Chen and L.W. Lin, MEMS fabrication based on nickel-nanocomposite: film deposition and characterization, J. Micromech. Microeng. 15 (2005) 2205-2215.

[42] T. Wang and K. W Kelly, Particulate strengthened Ni–Al2O3 microcomposite HARMs for harsh-environmental micromechanical applications. J. Micromech. Microeng, 15 (2005) 81–90.

[43] Y. Gan, D.Y. Lee and et al., Structure and properties of electrodeposited Cu-Al2O3 Nanocomposite thin films, Journal of Engineering Materials and Technology, 127 (2005) 451-456.

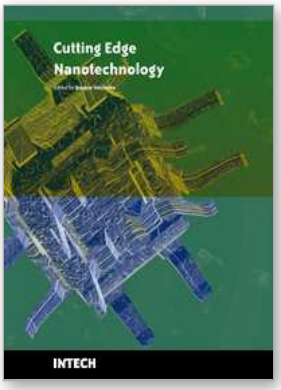

Cutting Edge Nanotechnology

Edited by Dragica Vasileska

ISBN 978-953-7619-93-0
Hard cover, 444 pages
Publisher InTech
Published online 01, March, 2010
Published in print edition March, 2010

The main purpose of this book is to describe important issues in various types of devices ranging from conventional transistors (opening chapters of the book) to molecular electronic devices whose fabrication and operation is discussed in the last few chapters of the book. As such, this book can serve as a guide for identifications of important areas of research in micro, nano and molecular electronics. We deeply acknowledge valuable contributions that each of the authors made in writing these excellent chapters.

InTech Europe
University Campus STeP Ri
Slavka Krautzeka 83/A
51000 Rijeka, Croatia
Phone: +385 (51) 770 447
Fax: +385 (51) 686 166
www.intechopen.com

InTech China
Unit 405, Office Block, Hotel Equatorial Shanghai
No.65, Yan An Road (West), Shanghai, 200040, China
中国上海市延安西路65号上海国际贵都大饭店办公楼405单元
Phone: +86-21-62489820
Fax: +86-21-62489821